# Theory, Implementation and Proof-of-Concept Study of Flight Safety 'Topology' Knowledge Maps for Accident Prediction and Prevention[1][2]

Ivan Y. Burdun
*Novosibirsk, Russia*

**Abstract:** *Flight safety 'topology' maps are intelligent formats designed to depict systemic knowledge of aircraft flight physics and logic in complex (multi-factor) situations. This knowledge is extracted from fast-time 'what-if' modeling and simulation (M&S) experiments. VATES tool (Virtual Autonomous Test and Evaluation Simulator, v.7/8) is employed as a 'knowledge generator'. A human pilot is not required in the simulator's flight control and scenario planning loops. However, a comprehensive 'parametric definition' of the aircraft/project of interest is a pre-requisite for obtaining valid results. These knowledge maps are used to support a 'bird's eye view' level depiction, analysis, prediction and protection of the aircraft's flight safety performance under uncertainty. The objective is to help reveal and avoid dangerous anomalies in the 'operator (pilot, automaton) – aircraft – operational environment' system behavior in advance, before the situation may become irreversible. Using this methodology, tactical goals and constraints of flight can be managed more coherently. The methodology helps the operator to find and apply a self-preserving knowledge-centered control tactics in a dynamic multi-factor flight situation. In the presented study, a broad set of flight cases comprising a human pilot's errors, onboard system failures and adverse weather conditions has been examined for a number of realistic operational hypotheses. Several characteristic topological objects that can either accelerate or slow down the recovery and mishap outcomes of a multi-factor situation have been identified. Results of examining a notional aircraft's safety performance in low-altitude flight in the presence of urban obstacles are presented as well. Principles of knowledge-centered pilot training and autonomous recovery control of aircraft in emergencies are demonstrated. Potential application areas include: aircraft aerodynamics design; intelligent flight control and flight envelope protection systems design; aircraft flight testing, certification and performance evaluation; situational training of line pilots, test pilots and pilot instructors; mission planning and flight operation.*

**Keywords:** flight safety, mapping and protection.

## 1. Introduction

### 1.1. Problem

*Multi-Factor Flight Situations*

A complex (multi-factor) situation can spontaneously develop in apparently normal flight as a result of dynamic mixing, cross-coupling of several unfavorable circumstances. There are four groups of operational (and design) factors that contribute to the development of a complex situation in flight:

(1) a human pilot's errors, inattention or deliberately unsafe actions, variations of a piloting tactics
(2) onboard equipment mechanical failures, data and logic errors
(3) demanding weather and terrain conditions (wind-shear, cross-wind, rain, wet runway, turbulence, natural and urban obstacles, etc.), and
(4) variations of the flight mission and aircraft data (configuration, C.G. position, flying mode, etc.).

*Knowledge System Shortcomings*

In spite of a negligibly small probability of occurrence, multi-factor accidents do happen in flight operation. Their logical and physical patterns are very unusual, rarely observed and poorly documented[1]. Many possible multi-factor accident scenarios are not known yet. Recorded cases can be grouped as follows: loss of control (LOC), controlled flight into terrain (CFIT), mid-air collisions, and use of a civil aircraft by terrorists as a weapon of mass destruction.


[2] This is an updated and expanded version of the paper submitted to the EWHSFF-2005 Conference, Beijing, P.R. China. Obsolete affiliation removed.

The root cause of the operator's failure under complex operational conditions is hidden in the gaps and other structural flaws of its 'internal knowledge base', which describes a multi-factor flight situation domain. These defects increase the risk of spontaneous development of a 'chain reaction' accident under multi-factor conditions[1, 2].

*Problem Formulation*

There exists a sub-domain of theoretically implausible but practically viable multi-factor accident patterns. At present, these scenarios cannot be blocked or remedied reliably in operation. Multi-factor cases are difficult to examine exhaustively during design, test and evaluation due to combinatorial, technical, time and budget constraints. A generalized yet affordable safety research and protection methodology is obviously needed.

### 1.2. Solution Approach

*Component Techniques*

A generalized approach has been developed to help enhancing aircraft safety under multi-factor conditions by exploring and mapping key physical and logical relationships of flight. The following disciplines, tools and processes are used in concert: aerodynamics, flight dynamics, complex flight situation theory, situational control, artificial intelligence (AI), graph theory, dynamic data structures, numeric techniques, mathematical modeling, simulation experiments, computer graphics, VATES (Virtual Autonomous Test and Evaluation Simulator)[2] proprietary software tool, Pentium-IV PC, MS Windows, MS Office, Pfe, MAGE, etc.

*Research Task Formulation*

The research task can be formulated as follows: (1) develop a methodology capable of deriving *a priori* systemic knowledge that represents key relationships of flight on a 'bird's eye view' level for a broad range of potentially unsafe multi-factor flight scenarios, (2) design a set of anthropomorphic formats to help 'implant' this knowledge into a specialist's long-term memory, and (3) carry out a proof-of-concept case study to demonstrate the feasibility of a knowledge-centered technology for flight safety prediction and protection.

*Disclaimer*

In this study, a generic model of the 'operator (pilot, automaton) – aircraft – operational environment' system behavior is employed as a 'virtual test article'. A 'parametric definition' of a notional commuter airplane is used. M&S results do not represent any particular flight accident or incident. The paper does not contain any vehicle- or case-specific safety recommendations for immediate use in flight operation.

## 2. Conceptual Framework

A generalized conceptual framework has been developed for an aircraft's safety performance mapping, analysis, prediction and protection under multi-factor conditions. These concepts are independent of aircraft type, flight mission, situation and operational conditions. In this section, a brief introduction of this theory will be made.

### 2.1. List of Concepts

Following is a list of concepts developed for studying operational safety of a complex flight situation domain[1,2]: micro- and macro-structure of flight, system model, VATES, system variable, state vector, event, process, scenario, 'flight', fuzzy constraint, safety color, safety palette, partial and integral safety spectra, safety chances, situation complexity index, safety index, situation complexity and safety build-up diagrams, event time-history diagram, fuzzy constraint violation/ restoration chronology diagram, basic situation scenario, operational (design) factor, operational hypothesis, situational tree, 'scenario – operational hypothesis' composition, safety chances distribution pie chart, total flight time of a situational tree, tree's cause-and-effect diagram, tree's specialization and competence measures, safety

classification categories, equal-safety cluster, safety window, safety 'topology', safety 'topology' objects, safety 'topology' maps, family of integral safety spectra of a situational tree, situational 'forest', family of flight safety windows for a situational 'forest', dynamic safety window, dynamic safety chances distribution chart, characteristic states of flight safety 'topology', flight safety 'topology' characteristics, and some other notions.

## 2.2. Safety 'Topology' Related Notions

*M&S Data Measurement*

The system behavior is described as a chronologically ordered sequence-set of *system states* $\boldsymbol{x}(t)$, $\boldsymbol{x}(t) = \{x_1(t), \ldots, x_i(t), \ldots, x_{N(\boldsymbol{x})}(t)\}$, where $x_i$ is a *system variable*, $x_i \in \boldsymbol{x}$, $t \in [t_*; t^*]$. This sequence is called a '*flight*' $\boldsymbol{F}_k$, $\boldsymbol{F}_k = \{\{x_1(t_*), \ldots, x_{N(\boldsymbol{x})}(t_*)\}, \ldots, \{x_1(t_* + (n-1)\cdot\Delta), \ldots, x_{N(\boldsymbol{x})}(t_* + (n-1)\cdot\Delta)\}\}$, where $n$ is the total number of records in $\boldsymbol{F}_k$, $t^* = t_* + (n-1)\cdot\Delta$, and $\Delta$ is the time increment of M&S data recording in a set $\boldsymbol{F}$.

*Micro- and Macro-Structure of Flight*

Safety related knowledge of a complex flight domain is constructed on two interconnected levels[1, 2]. These are the '*micro-structure*' of flight (a flight situation scenario) and the '*macro-structure*' of flight (a situational tree). The relationship between these two knowledge models is depicted in Fig. 1. A flight situation scenario is a directed graph which consists of events (vertices) and processes (arcs). A situational tree consists of branches ('flights'). The main branch (*trunk*) implements a given *basic situation scenario*, and a secondary $n^{\text{th}}$-order (derivative) branch represents a *multi-factor situation scenario* which is some meaningful variation of the basic scenario.

*Operational (Design) Factor*

The *operational (or design) factor* $\boldsymbol{\Phi}$ is some event or process (or its attribute), which can be added to or withdrawn from a basic scenario. Operational factors can vary substantially and independently, and thus improve or deteriorate flight safety. Normally, each factor $\boldsymbol{\Phi}$ is described by one system variable $x_i$, $x_i \in \boldsymbol{x}$. Operational factors are used in M&S experiments to create 'neighboring' multi-factor cases – specially designed variations of a basic situation. Each derivative 'flight' from a situational tree corresponds to one combination of operational factors $\boldsymbol{\Phi}_j$.

*Operational Hypothesis*

The *operational hypothesis* $\boldsymbol{\Gamma}$ is a formal rule used to incorporate a new combination of operational factors into the basic scenario. Any operational hypothesis can be defined as follows: $\tilde{\mathbf{A}} = \prod_{i=1}^{n}\left[\sum_{k=1}^{m}\hat{\mathbf{O}}^{i}_{k}\right]$, where $\boldsymbol{\Phi}^{i}_{k}$ is the $k^{\text{th}}$ dependent factor added to the basic scenario on the $i^{\text{th}}$ independent level of situational tree branching, $i = 1, \ldots, n$, $k = 1, \ldots m$; $\Pi$ is the symbol of Cartesian product; $\Sigma$ is the symbol of dependent combination of factor values $\Phi^{i}_{k}$ on the $i^{th}$ level. Therefore, the rule $\boldsymbol{\Gamma}$ can be viewed as a situational tree's 'genotype' which determines its shape, size and branching properties.

*Situational Tree*

A composition of a basic situation scenario $\mathbf{S}$ and operational hypothesis $\boldsymbol{\Gamma}$ in a M&S experiment, $\mathbf{S}\cdot\boldsymbol{\Gamma}$, results in a set of 'neighboring' situations ('flights'). This set is called the *situational* ('*what-if*') *tree* $\boldsymbol{T}$, $\boldsymbol{T} = \mathbf{S}\cdot\boldsymbol{\Gamma} \equiv \Omega(\boldsymbol{F})$. Each situation-branch $\boldsymbol{B}_k$ (a 'flight' $\boldsymbol{F}_{ik}$), $\boldsymbol{B}_k \in \boldsymbol{T}$, is defined by a subset of contributing factors $\boldsymbol{\Phi}_j$ (a rule $\boldsymbol{\Gamma}$), basic scenario $\mathbf{S}$ and the system dynamics. The goal of constructing situational trees is to examine combined effects of various operational (and possibly design) factors on an aircraft's safety performance and thus generate missing statistics on multi-factor accident patterns in advance.

*Pilot's 'Internal Situational Tree'*

It can be argued that a human pilot's situational (tactical) experience is stored in his/her long-term memory in the form of a 'situational tree'. As a fruit tree, a human pilot's internal 'situational tree' requires special care. This process

includes shaping of the tree's 'crown', 'grafting' of useful branches, reconstruction of lost or missing components, cutting of useless shoots, and other procedures. The goal is to obtain, for a given aircraft type and flight mission, a competent, efficient yet economic and quickly accessible system of knowledge that corresponds to a domain of anticipated complex (multi-factor) flight conditions.

The growth dynamics of a fractal tree shown in Fig. 2 is an ideal model illustration of a multi-stage process of the situational experience development in a human pilot's long-term memory. Characteristic levels of a human pilot's expertise and its transformation due to time are exemplified for ten notional 'life-cycle' steps, $k = 1, \ldots, 10$: $k \in \{1, 2, 3\}$ – experience of a student pilot, $k \in \{8, 9, 10\}$ – experience of a professional pilot (ace or test pilot), $k \in \{4, \ldots, 7\}$ – interim (immature) levels of experience. Fig. 3 depicts a natural tree, which can be used as a model of key structural and logical defects of a human pilot's situational experience knowledge base: missing knowledge, forgotten or shadowed knowledge, unsystematic knowledge, and fragmentary knowledge.

*Safety Classification Categories*

In order to measure the safety performance of a multi-factor flight situation domain in overall, a generalized 'safety ruler' that consists of five *safety classification categories*, **I**, …, **V**, is introduced[1,2]. These categories define *safe* (**I**), *conditionally safe* (**II**), *potentially dangerous* (**III**), *dangerous or prohibited* (**IV**), and *catastrophic, 'chain-reaction' type* (**V**) situations. The classification principle takes into account the palette, 'weight' and position of the four *basic safety colors*[1,2] $\{\xi_G, \xi_Y, \xi_R, \xi_B\}$ in the *integral safety spectrum* $\mathbf{\Sigma}$ of each 'flight' $\boldsymbol{F}_{ik}, \boldsymbol{F}_{ik} \in \Omega(\boldsymbol{F})$.

*Equal-Safety Clusters*

Any tree of 'neighboring' situations ('flights') can be partitioned onto six *disjoint equal-safety clusters*[1]: $\{K^{\mathbf{I}}, K^{\mathbf{II\text{-}a}}, K^{\mathbf{II\text{-}b}}, K^{\mathbf{III}}, K^{\mathbf{IV}}, K^{\mathbf{V}}\}$. The decomposition is performed automatically. The partitioning criteria for these six clusters are defined in[1,2]. For each safety classification category, a unique Roman digit $i$, $i \in \{\mathbf{I}, \ldots, \mathbf{V}\}$, and basic safety color $\xi^{\boldsymbol{i}}$, $\xi^{\boldsymbol{i}} \in \{\xi^{\mathbf{I}}, \ldots, \xi^{\mathbf{V}}\}$ are assigned, $\xi^{\mathbf{I}} \equiv \xi_G$, $\xi^{\mathbf{II\text{-}b}} \equiv \xi_Y$, $\xi^{\mathbf{IV}} \equiv \xi_R$, $\xi^{\mathbf{V}} \equiv \xi_B$, where $\xi^{\mathbf{II\text{-}a}}$ and $\xi^{\mathbf{III}}$ are interim colors: '*light-green*' and '*orange*'.

*Safety Chances Distribution*

A *distribution of safety chances* $\{\chi^{\mathbf{I}}, \chi^{\mathbf{II\text{-}a}}, \chi^{\mathbf{II\text{-}b}}, \chi^{\mathbf{III}}, \chi^{\mathbf{IV}}, \chi^{\mathbf{V}}\}$ can be calculated for the six clusters of neighboring situations which constitute a situational tree $\boldsymbol{T}$: $(\forall j)\ (j = \mathbf{I}, \ldots, \mathbf{V})\ (n^j = 0)\ (\forall \boldsymbol{F}_k)\ (\boldsymbol{F}_k \in \{\boldsymbol{F}_1, \ldots, \boldsymbol{F}_{N(\boldsymbol{T})}\} \wedge N(\boldsymbol{T}) \neq 0)$
$(\boldsymbol{F}_k \in \mathrm{K}^j \Rightarrow n^j = n^j + 1) \wedge (\chi^j = \dfrac{n^j}{N(\boldsymbol{T})} \cdot 100, \sum_{j=\mathbf{I}}^{\mathbf{V}} \chi^j = 100\%)$, where $n^j$ is the counter of situations in the cluster $K^j$.

*Safety Window*

Let us have a tree of 'flights' $\Omega(\boldsymbol{F})$, $\Omega(\boldsymbol{F}) = \{\boldsymbol{F}_{(1),(1)}, \ldots, \boldsymbol{F}_{(i),(j)}, \ldots, \boldsymbol{F}_{(m),(n)}\}$ with the following pairs of values of two key operational factors $\mathbf{\Phi}_a$ and $\mathbf{\Phi}_b$: $\{(\Phi_{a(1)}, \Phi_{b(1)}), \ldots, (\Phi_{a(i)}, \Phi_{b(j)}), \ldots, (\Phi_{a(m)}, \Phi_{b(n)})\}$, where $\Phi_{a(1)} > \Phi_{a(2)} > \ldots > \Phi_{a(m)}$ is a top-to-bottom vertical ordering relation for values of the first factor $\mathbf{\Phi}_a$ and $\Phi_{b(1)} < \Phi_{b(2)} < \ldots < \Phi_{b(n)}$ is a left-to-right horizontal ordering relation for values of the second factor $\mathbf{\Phi}_b$. Then the *flight safety window* can be defined as a $m \times n$ matrix $W(\mathbf{\Phi}_a, \mathbf{\Phi}_b)$ with coordinates $\mathbf{\Phi}_a$ and $\mathbf{\Phi}_b$, where $w_{ij}$ is a cell located on the crossing of the row #$i$ and column #$j$, $w_{ij} = [(\Phi_{a(i)}, \Phi_{b(j)}), \xi^k_{ij}]$, $i = 1, \ldots, m$, $j = 1, \ldots, n$, $k \in \{\mathbf{I}, \ldots, \mathbf{V}\}$. The cell $w_{ij}$ contains the following information: (1) $(\Phi_{a(i)}, \Phi_{b(j)})$ – a pair of values of factors $(\mathbf{\Phi}_a, \mathbf{\Phi}_b)$, where $\Phi_{a(i)} = const$ for $(\forall i)$ $(i = 1, \ldots, m)$ and $\Phi_{b(j)} = const$ for $(\forall j)$ $(j = 1, \ldots, n)$, and (2) $\xi^k_{ij}$ – the color of the $k^{\text{th}}$ cluster which the 'flight' $\boldsymbol{F}_{(i),(j)}$ belongs to, $k \in \{\mathbf{I}, \ldots, \mathbf{V}\}$, $\xi^k_{ij} \in \{\xi^{\mathbf{I}}, \ldots, \xi^{\mathbf{V}}\}$. An algorithm has been developed for mapping 'flights' from $\Omega(\boldsymbol{F})$, $\Omega(\boldsymbol{F}) = \mathbf{S} \cdot \mathbf{\Gamma}$, on to a safety window $W(\mathbf{\Phi}_a, \mathbf{\Phi}_b)$.

*Flight Safety 'Topology'*

Given a tree $\Omega(\boldsymbol{F})$, $\Omega(\boldsymbol{F}) = \mathbf{S} \cdot \mathbf{\Gamma}$, and its safety window $W(\mathbf{\Phi}_a, \mathbf{\Phi}_b)$, the aircraft's safety performance can be graded according to the categories $\{\mathbf{I}, \ldots, \mathbf{V}\}$[1,2] where $\mathbf{\Phi}_a, \mathbf{\Phi}_b \in \{\mathbf{\Phi}_{j(1)}, \ldots, \mathbf{\Phi}_{j(N(\mathbf{\Phi}))}\}$. Then, in the window $W(\mathbf{\Phi}_a, \mathbf{\Phi}_b)$ the following *characteristic topological objects* can be identified (Fig. 4):

- the 'abyss' **1** (a catastrophe)

- the 'hill' **2** (a danger)
- the 'slope' **3** (a reversible state transition)
- the 'valley' **4** (standard safety situations)
- the 'lake' **5** (maximum safety, or optimum situations), and
- the 'precipice' **6** (abrupt, irreversible state transitions, 'chain reaction').

An integrated color graphic image of the mutual arrangement and inter-dependence of the above-listed objects in the window $W(\mathbf{\Phi}_a, \mathbf{\Phi}_b)$ is called the *safety 'topology'* of a multi-factor flight situation domain with two key operational factors $(\mathbf{\Phi}_a, \mathbf{\Phi}_b)$ selected for monitoring.

*Definition of Safety 'Topology' Objects*

The '*abyss*' is a subset of neighboring – in projection on the window $W(\mathbf{\Phi}_a, \mathbf{\Phi}_b)$ plane – 'flights', which represent catastrophic scenarios. These situations are classified as Category **V** cases and painted in black color $\xi^{\mathbf{V}}$. The '*hill*' is a subset of neighboring – in projection on the window $W(\mathbf{\Phi}_a, \mathbf{\Phi}_b)$ plane – 'flights', which are known as dangerous scenarios. These situations are classified as Category **IV** cases and painted in red color $\xi^{\mathbf{IV}}$. The '*slope*' or '*foot*' is a subset of transitional situations, which link together a 'valley' and a 'hill' – smoothly and by a shortest way – in projection on the window $W(\mathbf{\Phi}_a, \mathbf{\Phi}_b)$ plane. They are classified as Category **II-b** and **III** cases: $((\xi^{\mathbf{I}} \vee \xi^{\mathbf{II\text{-}a}}) \rightarrow (\xi^{\mathbf{II\text{-}b}} \vee \xi^{\mathbf{III}}) \rightarrow (\xi^{\mathbf{IV}})) \Rightarrow$ '*slope*'. Normally, the 'slope'-type situations are reversible; they must be known and routinely managed in flight operations.

The '*valley*' is a subset of neighboring – in projection on the window $W(\mathbf{\Phi}_a, \mathbf{\Phi}_b)$ plane – 'flights' which represent standard, normal safety scenarios. They are classified as Category **I** and **II-a** cases and painted in green and light-green colors ($\xi^{\mathbf{I}}$, $\xi^{\mathbf{II\text{-}a}}$), respectively. The '*lake*' is a subset of neighboring – in projection on the window $W(\mathbf{\Phi}_a, \mathbf{\Phi}_b)$ plane – 'flights', which are considered as optimal scenarios maximizing the vehicle's safety performance or mission effectiveness. Normally, they belong to Category **I** and **II-a** cases and are painted in turquoise color $\xi_{\mathrm{T}}$. Finally, the '*precipice*' is a subset of abrupt transitions from a 'valley'/'hill' to an 'abyss'. They are classified as Category **V** cases and represent catastrophic developments of flight: $(((\xi^{\mathbf{I}} \vee \xi^{\mathbf{II\text{-}a}}) \rightarrow \xi^{\mathbf{V}}) \vee (\xi^{\mathbf{IV}} \rightarrow \xi^{\mathbf{V}})) \Rightarrow$ '*precipice*'. The precipice type transitions are irreversible, i.e. prone to a 'chain reaction' accident. Therefore, they must be reliably prevented (avoided) in flight operations and their precursors must be known.

*Dynamic (Time-Dependent) Safety Window*

It is assumed that an aircraft is equipped with multi-modal sensors capable of real-time measurements of two key factors $(\mathbf{\Phi}_a, \mathbf{\Phi}_b)$ and a third, possibly time-critical, key factor $\mathbf{\Phi}_c$. Then a sequence of safety windows $W(\mathbf{\Phi}_a, \mathbf{\Phi}_b)|t_0$, $W(\mathbf{\Phi}_a, \mathbf{\Phi}_b)|t_1$, $W(\mathbf{\Phi}_a, \mathbf{\Phi}_b)|t_2$, …, can be constructed for a series of consecutive flight time instants $\{t_0, t_1, t_2, \ldots\}$. This sequence, $W(\mathbf{\Phi}_a, \mathbf{\Phi}_b)|t_i \wedge \Phi_c = \mathbf{\Phi}_c(t_i)$, $t_i = t_0, t_1, t_2, \ldots$, is called the *dynamic (time-dependent) safety window*, $W(\mathbf{\Phi}_a, \mathbf{\Phi}_b, \mathbf{\Phi}_c) = f(t)$. It maps additional effects of the time-critical factor $\mathbf{\Phi}_c$ on the aircraft's safety performance under the operational hypothesis $\mathbf{\Phi}_a \times \mathbf{\Phi}_b$. A virtual environment that ergonomically implements the sequence $W(\mathbf{\Phi}_a, \mathbf{\Phi}_b, \mathbf{\Phi}_c) = f(t)$ in fact represents an intelligent pilot-vehicle interface system suitable for active real-time safety management under multi-factor conditions.

*'Last Chance for Recovery' Point*

Given a preset *flight safety prediction time range* $[t_0; t_0 + \Delta^{\mathrm{P}}]$, $[t_0; t_0 + \Delta^{\mathrm{P}}] \subset [t_*; t^*]$, and a triple of key factors $\{\mathbf{\Phi}_a, \mathbf{\Phi}_b, \mathbf{\Phi}_c\}$, $\{\mathbf{\Phi}_a, \mathbf{\Phi}_b, \mathbf{\Phi}_c\} \subset \Omega(\mathbf{\Phi})$, a sub-tree $\boldsymbol{T}'$ that emerges from the current situation can be extracted from $\boldsymbol{T}$ and processed onboard, where $t_0$ is the *safety prediction starting point* measured with respect to the current flight time $t$ and $\Delta^{\mathrm{P}}$ is the *depth of safety predictions*, $\Delta^{\mathrm{P}} \in [3; 30]$ s. Then for the situations from $\boldsymbol{T}'$ it becomes possible to calculate the probability $(\chi^{\mathbf{IV}} + \chi^{\mathbf{V}})$ of the event that the system state will enter the zones $\xi^{\mathbf{IV}}$ and $\xi^{\mathbf{V}}$ during the prediction time range $[t_0; t_0 + \Delta^{\mathrm{P}}]$. If $(\chi^{\mathbf{IV}} + \chi^{\mathbf{V}}) > \chi_{\max}$ this means that a catastrophic development of the current situation is imminent, where $\chi_{\max}$ is the *threshold for safety protection decision-making*.

The value of $\chi_{max}$ determines the *'last chance for recovery' point* $t_{\uparrow}$ [1,2]. At this point, it is mandatory for the operator to abort any current automatic control or piloting tactics and immediately implement a new control scenario for restoring flight safety. It is essential that short-term safety forecasts and recovery control selection decisions are based on the systematic knowledge of flight physics and logic stored in the situational tree $\boldsymbol{T}$.

*Safety Restoring Scenario*

Given an emergency, a *safety restoring (recovery control) scenario* $\mathbf{S}_{\uparrow}$ must be applied to the aircraft beginning from the 'last chance for recovery' point $t_{\uparrow}$. This is a scenario of the safest possible branch from $\boldsymbol{T}'$ that continues the current situation and moves the vehicle away from 'abyss' type transitions in the safety window. The scenario $\mathbf{S}_{\uparrow}$ can be implemented either automatically or manually. This depends on the complexity level of a current situation, mission type, aircraft class and technical condition, phase of flight, operator qualification (competence) and physical (technical) condition, etc. In the manual recovery mode, key parameters of the safety restoring scenario $\mathbf{S}_{\uparrow}$ can be entered by means of a tactile display containing a dynamic window $W(\boldsymbol{\Phi}_a, \boldsymbol{\Phi}_b, \boldsymbol{\Phi}_c(t))$ or using other advanced pilot-vehicle interface technologies[1]. In the automatic recovery mode, these parameters are derived from the onboard knowledge base – a *'forest' of situational trees*, $\Omega(\boldsymbol{T})$.

*Active Safety Management*

A generic *algorithm for active safety management* during flight under multi-factor conditions has been developed[1,2] using the formal framework introduced above. The algorithm's input data set includes the following: $\{\Omega(\boldsymbol{T}), \Omega(\boldsymbol{\Phi}), \Omega(\boldsymbol{\Gamma}), \Omega^{M}(\boldsymbol{\Phi}), \{\boldsymbol{\Phi}_a, \boldsymbol{\Phi}_b, \boldsymbol{\Phi}_c\}, \Omega(\boldsymbol{C}), \boldsymbol{x}', t_0, \Delta^{P}, \boldsymbol{T}', \chi^{IV}, \chi^{V}, \ldots\}$, where $\Omega^{M}(\boldsymbol{\Phi})$ is a subset of key operational factors selected for real-time monitoring and aircraft's safety performance prediction during a given phase of flight, $\Omega^{M}(\boldsymbol{\Phi}) = f(t)$, $\{\boldsymbol{\Phi}_a, \boldsymbol{\Phi}_b, \boldsymbol{\Phi}_c\} \subset \Omega(\boldsymbol{\Phi})$, $\boldsymbol{\Phi}_a, \boldsymbol{\Phi}_b, \boldsymbol{\Phi}_c = f(t)$, $\Omega(\boldsymbol{C})$ is a set of monitored fuzzy constraints, $\boldsymbol{T}' \subset \boldsymbol{T}$, and $\boldsymbol{x}'$ is a subset of key monitored system variables, $\boldsymbol{x}' \subset \boldsymbol{x}$. By tuning these parameters (primarily, $\Omega(\boldsymbol{\Gamma})$, $\Omega^{M}(\boldsymbol{\Phi})$, $\{\boldsymbol{\Phi}_a, \boldsymbol{\Phi}_b, \boldsymbol{\Phi}_c\}$, $t_0$ and $\Delta^{P}$), a flexible, individualized policy of active flight safety management can be tailored to account for the intelligence strengths and weaknesses of a specific human pilot or automaton type.

## 3. Simulation Results and Discussion

A series of M&S experiments has been carried out with the system model for takeoff, climb, level and descent flight modes of a notional commuter airplane using the methodology described in Section 2.

### 3.1. Experiment Setup and Statistics

Some 1500 multi-factor situations have been examined for a number of realistic operational hypotheses. Six basic scenarios $\{\mathbf{S}_1, \ldots, \mathbf{S}_6\}$ have been constructed and simulated. This list includes the following ones: 'Normal takeoff, benign weather' ($\mathbf{S}_1$), 'Normal takeoff, cross-wind' ($\mathbf{S}_2$), 'Continued takeoff, one engine out' ($\mathbf{S}_3$), 'Normal takeoff, wind-shear' ($\mathbf{S}_4$), 'Continued takeoff, one engine out and cross-wind' ($\mathbf{S}_5$), and 'Low-altitude climb, level flight and descent in the presence of urban infra-structure obstacles' ($\mathbf{S}_6$). In overall, 20 fuzzy constraints have been defined for monitoring and to assess the vehicle's safety performance for a subset $\boldsymbol{x}'$ of key system variables $x_k, \boldsymbol{x}' = \{V_{IAS}, \beta, n_z, E, N, \gamma, \vartheta, V_{zg}, \alpha, k_{LG}, \delta_e, \delta_a, \delta_r, \delta_F, \ldots\}$.

The following operational factors have been selected for testing in association with the basic scenarios $\mathbf{S}_1, \ldots, \mathbf{S}_6$: $\boldsymbol{\Phi}_1$ – the C.G. position ($\bar{x}_{CG}$); $\boldsymbol{\Phi}_2$ – the rotation airspeed ($V_R$); $\boldsymbol{\Phi}_3$ – the elevator increment for rotation ($\Delta\delta_e$); $\boldsymbol{\Phi}_4$ – the 'wheels – runway surface' adhesion factor ($\mu$); $\boldsymbol{\Phi}_5$ – the cross-wind velocity ($W_{yg}$); $\boldsymbol{\Phi}_6$ – 'flaps-up' start altitude ($H_{FL}$); $\boldsymbol{\Phi}_7$ – the commanded flight path angle, flaps extended ($\theta_{G1}$); $\boldsymbol{\Phi}_8$ – the commanded flight path angle, flaps retracted ($\theta_{G2}$); $\boldsymbol{\Phi}_9$ – the wind-shear intensity ($k_W$); $\boldsymbol{\Phi}_{10}$ – the engines power rating at takeoff ($k_P$); $\boldsymbol{\Phi}_{11}$ – the commanded bank angle ($\gamma_G$); $\boldsymbol{\Phi}_{12}$ – the 'engine out' airspeed ($V_{EF}$); and $\boldsymbol{\Phi}_{13}$ – the left-hand engine 'inoperative' or 'operative' status at $V_{EF}$ ($\xi_{LHE}$).

By logically combining these factors, 14 realistic operational hypotheses have been designed, i.e. $\Omega(\boldsymbol{\Gamma}) = \{\boldsymbol{\Gamma}_1, \ldots, \boldsymbol{\Gamma}_{14}\}$. In overall, the following compositions of basic takeoff scenarios $\mathbf{S}_i$ and operational hypotheses $\boldsymbol{\Gamma}_k, \boldsymbol{\Gamma}_k \in \Omega(\boldsymbol{\Gamma})$, have been

examined in M&S: $\mathbf{S}_1\cdot\mathbf{\Gamma}_1$, $\mathbf{S}_2\cdot\mathbf{\Gamma}_2$, $\mathbf{S}_1\cdot\mathbf{\Gamma}_3$, $\mathbf{S}_1\cdot\mathbf{\Gamma}_4$, $\mathbf{S}_3\cdot\mathbf{\Gamma}_5$, $\mathbf{S}_4\cdot\mathbf{\Gamma}_6$, $\mathbf{S}_4\cdot\mathbf{\Gamma}_7$, $\mathbf{S}_1\cdot\mathbf{\Gamma}_8$, $\mathbf{S}_1\cdot\mathbf{\Gamma}_9$, $\mathbf{S}_5\cdot\mathbf{\Gamma}_{10}$, $\mathbf{S}_1\cdot\mathbf{\Gamma}_{11}$, $\mathbf{S}_4\cdot\mathbf{\Gamma}_{12}$, $\mathbf{S}_4\cdot\mathbf{\Gamma}_{13}$ and $\mathbf{S}_6\cdot\mathbf{\Gamma}_{14}$. Presented below are results of the M&S experiments carried out for six hypotheses from this list, namely: $\mathbf{\Gamma}_2 = W_{yg} \times \mu$, $\mathbf{\Gamma}_6 = k_W \times H_{FL}$, $\mathbf{\Gamma}_7 = \overline{x}_{CG} \times k_W \times (\theta_{G1} + \theta_{G2})$ $(\overline{x}_{CG} = \overline{x}_{CG\min})$, $\mathbf{\Gamma}_{10} = \xi_{LHE} \times V_{EF} \times W_{yg}$ $(\xi_{LHE} = 0)$, $\mathbf{\Gamma}_{12} = k_W \times \theta_{G1} \times \gamma_G$ $(k_W = 1)$, and $\mathbf{\Gamma}_{14} = \theta_{G2} \times \gamma_G$.

## 3.2. Examples of Takeoff Safety Topology Mapping and Analysis

In Fig. 5, flight safety windows and safety chances distributions are shown for five takeoff compositions: $\mathbf{S}_2\cdot\mathbf{\Gamma}_2$, $\mathbf{S}_4\cdot\mathbf{\Gamma}_6$, $\mathbf{S}_4\cdot\mathbf{\Gamma}_7$, $\mathbf{S}_5\cdot\mathbf{\Gamma}_{10}$ and $\mathbf{S}_4\cdot\mathbf{\Gamma}_{12}$. In particular, the safety window $W$ ($\mathbf{\Phi}_4$, $\mathbf{\Phi}_5$), where $\mathbf{\Phi}_4 \equiv \mu$ and $\mathbf{\Phi}_5 \equiv W_{yg}$, constructed for the composition $\mathbf{S}_2\cdot\mathbf{\Gamma}_2$ contains one central green 'valley', two side red 'hills' and two connecting 'slopes'. A steep 'slope' is observed in a ground-roll motion mode for dry and semi-wet runway surface conditions. A more gradual transition between safe and unsafe situations can be noticed for wet and water-covered runways. The shape and position of a 'cross-wind velocity – adhesion factor' operational constraint are visually identifiable. Scenario variants with strong cross-wind velocities of |15|…|20| m/s can be dangerous during ground-roll. These cases constitute 45% of all the cases constituting $\mathbf{S}_2\cdot\mathbf{\Gamma}_2$. The remaining situations are safe and belong to Categories **I** and **II**.

In the composition $\mathbf{S}_4\cdot\mathbf{\Gamma}_6$, the safety window $W$ ($\mathbf{\Phi}_9$, $\mathbf{\Phi}_6$) maps a sub-domain of takeoff situations under severe unsteady wind conditions. In the scenario $\mathbf{S}_4$, the commanded flight path angles are: $\theta_{G1}/\theta_{G2} = 8^o/8^o$. If a 'strong' or worse wind-shear is expected ($k_W \geq 1$) takeoff must be prohibited. In order to evaluate a possibility of safer outcomes at moderate wind-shear effects ($k_W < 1$), it is expedient to expand the flight safety window downward. If the wind-shear intensity increases from 'very strong' ($k_W > 1.4$) to 'hurricane' ($k_W = 2$), a 'precipice' type transition **6** is likely to occur at low 'flaps-up start' altitudes, $H_{FL} \in [60; 70]$ m. If the aircraft unintentionally enters a zone of 'very strong' wind-shear with $k_W = 1.2 \ldots 1.6$, flaps must be retracted as late as possible to stay within the right-hand 'orange' zone. In overall, the chances of a catastrophic outcome for the operational domain $\mathbf{S}_4\cdot\mathbf{\Gamma}_6$ are high: $(\chi^{\mathbf{IV}} + \chi^{\mathbf{V}}) \approx 70\%$.

The safety 'topology' map of the composition $\mathbf{S}_4\cdot\mathbf{\Gamma}_7$ includes the following characteristic objects – ref. the window $W$ ($\mathbf{\Phi}_9$, $\mathbf{\Phi}_7 + \mathbf{\Phi}_8$) in Fig. 5: a small green 'valley' at a lower left-hand corner of the window, a wide ($\Delta\mathbf{\Phi}_9$ ($\xi^{\mathbf{III}}$) $\approx 0.6$) orange 'slope' above it followed by an extensive red 'hill' ($\chi^{\mathbf{IV}} = 37\%$) adjacent to a black 'abyss' at the upper right-hand corner. The most dangerous transition can occur at $\theta_{G1}/\theta_{G2} = 6^o/8^o$ if the wind-shear intensity increases from $k_W >$ 1.6 and higher. These observations can be useful to dynamically define robust tactical piloting goals and constraints for pairs ($\theta_{G1}$, $\theta_{G2}$) as a function of the wind-shear intensity. In particular, at takeoff under 'strong' and 'very strong' wind-shear ($1 < k_W \leq 1.6$) a maximum safety level is achieved at $\theta_{G1}/\theta_{G2} = 5^o/3^o$. It is prohibited to climb at $\theta_{G1}/\theta_{G2} > 7^o/5^o$, and irreversible transitions are likely to occur at $\theta_{G1} \geq 12^o$.

In the composition $\mathbf{S}_5\cdot\mathbf{\Gamma}_{10}$, the safety window $W$ ($\mathbf{\Phi}_{12}$, $\mathbf{\Phi}_5$) incorporates a wide central 'valley' and two side 'hills'. A large enough 'abyss' occupies the lower left-hand corner adjacent to the left-hand 'hill' and the central 'valley'. It is emerged at small and medium values of $V_{EF}$, $V_{EF} \in [100; 145]$ km/h, and is linked to the 'valley' by a 'precipice' type transitions **6**. A small 'abyss' is also revealed at a cross-wind velocity of about 18 m/s for $V_{EF} \in [175; 190]$ km/h.

It follows from the composition $\mathbf{S}_4\cdot\mathbf{\Gamma}_{12}$ (the window $W$ ($\mathbf{\Phi}_7$, $\mathbf{\Phi}_{11}$)) that a 'strong' wind-shear during initial climb can sharply degrade the aircraft's safety performance at small values of the commanded flight path angle ($\theta_{G1} \leq 4^o$). The safety 'topology' calculated for 'strong' wind-shear effects contains a stable catastrophic 'abyss' (a black strip in the bottom of $W$ ($\mathbf{\Phi}_7$, $\mathbf{\Phi}_{11}$)) and 'precipice' transitions **6** for small $\theta_{G1}$ and any commanded bank angle $\gamma_G$. It means that an attempt to perform initial climb at small commanded flight path angles ($2^o \ldots 4^o$) inevitably leads to a fatal outcome.

## 3.3. Case Study: Notional Low-Altitude Flight in the Presence of Urban Obstacles

Fig. 6 schematically depicts the flight paths, prediction sub-trees and safety windows constructed for two alternative scenarios of notional low-altitude flight in the presence of a tower-type urban obstacle of unknown location. This is a composition $\mathbf{S}_6\cdot\mathbf{\Gamma}_{14}$ which describes a sub-domain of climb, level flight and descent modes of a notional airliner flying in clean configuration at $V_{IAS} \in [320; 360]$ km/h and $H \in [200; 400]$ m. The resulting situational tree of $\mathbf{S}_6\cdot\mathbf{\Gamma}_{14}$ represents hypothetical situations with various combinations of the commanded flight path and bank angles: $\theta_{G2} \in \{-12^o, \ldots, +24^o\}$ and $\gamma_G \in \{-45^o, \ldots, +45^o\}$.

Two alternative scenarios are demonstrated: $\mathbf{S}_0 \cup \mathbf{S}_\downarrow$ and $\mathbf{S}_0 \cup \mathbf{S}_\uparrow$. They correspond to a terrorist- (or fool-) type control and safety protection AI control, respectively. The symbols $\mathbf{S}_0$, $\mathbf{S}_\downarrow$ and $\mathbf{S}_\uparrow$ stand for the following scenario segments: 'obstacle approach' ($\mathbf{S}_0$) with a discrete time scale $\{t_0, \ldots, t_7\}$, 'imminent collision' ($\mathbf{S}_\downarrow$) with a time scale $\{t_8, \ldots, t_{13}\}$, and 'collision avoidance' ($\mathbf{S}_\uparrow$) with a time scale $\{t_{14}, \ldots, t_{19}\}$. Four characteristic points of the decision-making process are shown as an example: $t_1$ – 'no obstacle ahead', $t_7$ – 'last chance for recovery', $t_{13}$ – 'just before impact', $t_{17}$ – 'minimum distance to obstacle', and $t_{19}$ – 'safety restoration complete'. Respectively, four states of the dynamic safety window $W(\mathbf{\Phi}_8, \mathbf{\Phi}_{11})$ are depicted for these time instants, where $W(\mathbf{\Phi}_8, \mathbf{\Phi}_{11}) \mid t_1 \equiv W(\mathbf{\Phi}_8, \mathbf{\Phi}_{11}) \mid t_{19}$.

Fig. 7 shows a discrete time-history of the dynamic safety window (fuzzified) $W(\mathbf{\Phi}_8, \mathbf{\Phi}_{11}) = f(t)$ constructed for two alternative scenarios: $\mathbf{S}_0 \cup \mathbf{S}_\downarrow$ – imminent collision and $\mathbf{S}_0 \cup \mathbf{S}_\uparrow$ – collision avoidance. A 'last chance for recovery' point $t_\uparrow$, $t_\uparrow \equiv t_7$, can be identified automatically using the following criterion: $(\theta_{G2}/\gamma_G\,(t-\Delta) \notin w|\xi^V \wedge \theta_{G2}/\gamma_G\,(t) \in w|\xi^V) \Rightarrow t = t_\uparrow$. Fig. 8 illustrates the principles of simple, color analysis based, search for a new safety restoring value-cell of the current tactical piloting goals (commanded flight path and bank angles) inside the safety window $W(\mathbf{\Phi}_8, \mathbf{\Phi}_{11})$. The search process is quick and can be performed automatically or manually. Instead of the old, collision-prone, goal ($\theta_{G2}/\gamma_G = -15^o/0^o$) the algorithm picks up a new one ($\theta_{G2}/\gamma_G = 6^o/30^o$) which is required to carry out an automatic or manual evasion maneuver. This new cell is close to the '*center of gravity*' of the right-hand '*island' of safe and conditionally safe scenarios* remaining in the window $W(\mathbf{\Phi}_8, \mathbf{\Phi}_{11}) \mid t_7$. Finally, Fig. 9 depicts a time-history of the flight safety chances distribution for the old ($\mathbf{S}_0 \cup \mathbf{S}_\downarrow$) and new ($\mathbf{S}_0 \cup \mathbf{S}_\uparrow$) flight control tactics. *Characteristic states of the aircraft safety dynamics*, {A, B, …, L}, are shown as well. They can be used in the recovery decision-making process.

## 4. Conclusion

A generalized methodology has been developed for mapping an aircraft's flight safety performance in complex (multi-factor) situations. Several types of safety 'topology' knowledge maps have been designed, implemented and demonstrated using VATES M&S tool. These intelligent formats can serve as a virtual medium for a 'bird's eye's view' level depiction, analysis and prediction of flight safety under uncertainty. In this process, both physics and logic of a multi-factor 'what-if neighborhood' built around a given basic situation is explored. The goal is to enhance the situational knowledge base and the decision-making mechanism of an operator (a pilot or automaton) in emergencies.

The proposed safety 'topology' maps are expedient to integrate with other advanced techniques and technologies, such as MDO systems, FMEA tools, vehicle health-monitoring systems, multi-modal sensors, and VR-technologies. The overall goal is to design reliable and affordable multi-function flight safety protection systems. These systems must be able to recognize and remedy both known and unknown yet complex flight accident patterns. This list includes (but not limited to) the following situation types: LOC, CFIT, 'pilot error', '9/11', midair collision, and other scenarios.

The developed methodology can be applied to the following problem fields: advanced examination of the combined effect of aerodynamics, flight control and operational factors on the aircraft flight dynamics and safety in design; knowledge-centered training of line pilots, test pilots and pilot instructors; design of terrorist-/ fool-proof aircraft safety protection systems; research into autonomous flight control under uncertainty and collision avoidance in close 'free flight' airspace.

## References

[1]Burdun, I.Y., 'Prediction of Aircraft Safety Performance in Complex Flight Situations' (Paper 2003-01-2988), *Proc. of the 2003 Advances in Aviation Safety Conference, September 8–12,* 2003*, Montreal*, SAE, 2003, 18 pp.

[2]Burdun, I.Y., Burdun, E.I., 'VATES – Virtual Autonomous Test and Evaluation Simulator' (Version 7 – Professional), User's Manual, 2000, 155 pp.

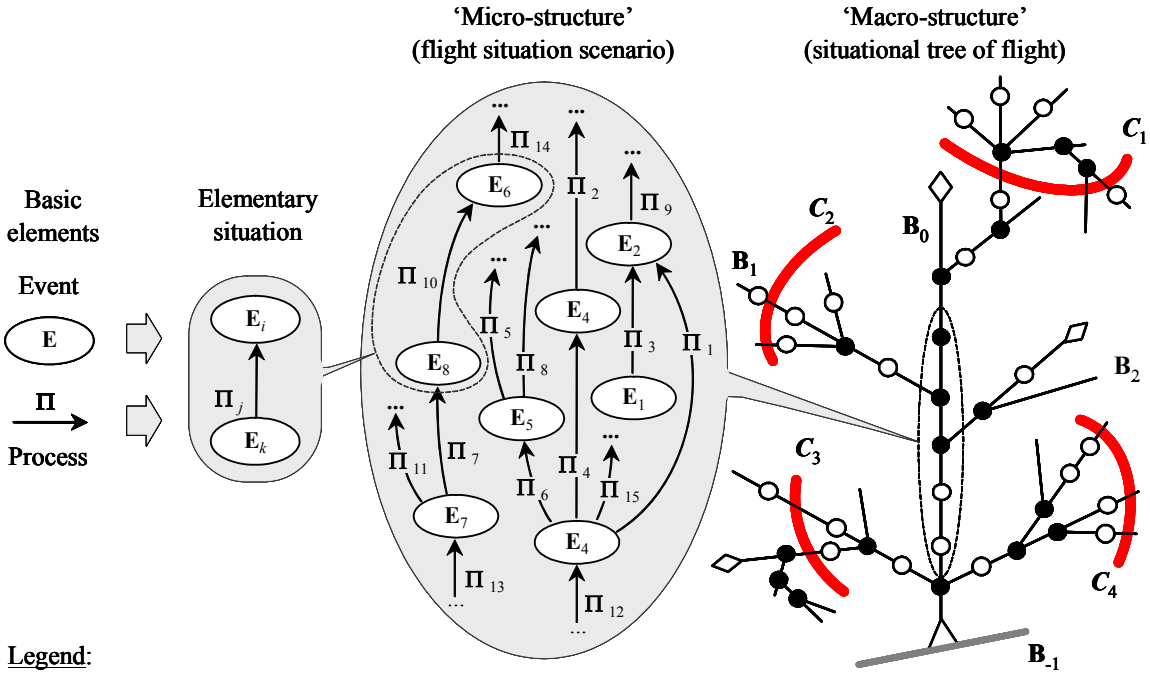


$\mathbf{E}_i$ – event; $\mathbf{\Pi}_j$ – process; $\boldsymbol{C}_m$ – fuzzy constraint; ○ – reference/ check state ('node'); ● – branch grafting state ('bud'); ◊ – branch's target state ('leaf'); Δ – branch's source state ('root'); $\mathbf{B}_{-1}$ – parent's branch; $\mathbf{B}_0$ – main branch ('trunk') – basic flight situation scenario; $\mathbf{B}_n$ – $n$-th order derivative branch – a complex flight situation scenario with $n$ contributing factors, $n = 1, 2, \ldots$

Fig. 1. 'Micro-' and 'macro-structure' of situational knowledge of flight

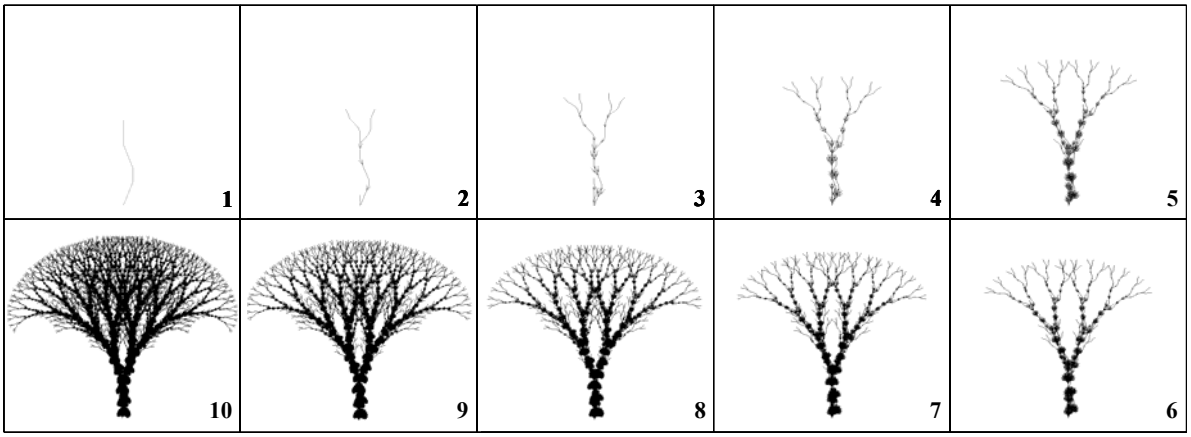


Legend: Fractal tree generating software: FracTree 1.0 program for MS Windows (shareware). Author: M. Schernau. Fractal name: Model of a human pilot's situational experience growth. Number of branching directions: 20. Axiom: -----G. Tree growth rules: G → [V]+FFX-F-FFX+FX[+G][-G]F, V → XF[G], X → F[-XF][+XF] FX. Characteristic levels of expertise: $k \in \{1, 2, 3\}$ – experience of a student pilot, $k \in \{8, 9, 10\}$ – experience of a professional pilot, ace, or test pilot, $k \in \{4, \ldots, 7\}$ – interim (immature) states of experience.

Fig. 2. Fractal tree growth dynamics as an ideal model of a human pilot's situational (tactical) experience development in the long-term memory

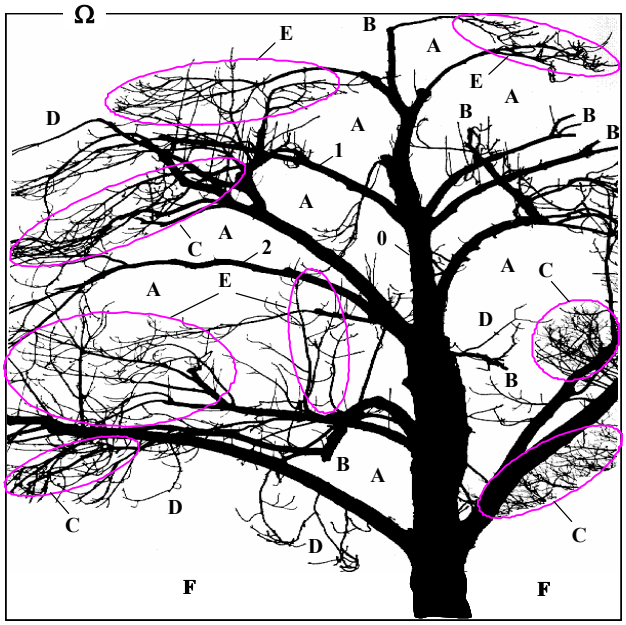


Legend:

| | Characteristic zone of a pilot's situational knowledge base | Natural tree based analogy |
|---|---|---|
| **Ω** | Space of possible complex flight situation scenarios | Space available for tree growth |
| **0** | Baseline (standard/non-standard) flight situation scenario | Tree's trunk |
| **1** | One-factor non-standard flight situation scenario | First-order derivative branch |
| **2** | Two-factor non-standard flight situation scenario | Second-order derivative branch |
| **A** | Missing knowledge | Absent though possible branching |
| **B** | Forgotten or shadowed knowledge | Dry or broken branches |
| **C** | Unsystematic knowledge | Excessive, chaotic branching |
| **D** | Fragmentary knowledge | Insufficient, sparse branching |
| **E** | Systematic knowledge | Optimally dense branching |
| **F** | Physically unattainable flight situation scenarios | A sub-domain where branching is impossible |

Note. This tree photo was made near Cranfield University's Social Club (England, Bedfordshire, Cranfield University Campus, autumn 1995)

Fig. 3. A natural tree based illustration of main structural and logical defects of a human pilot's situational (tactical) experience knowledge base

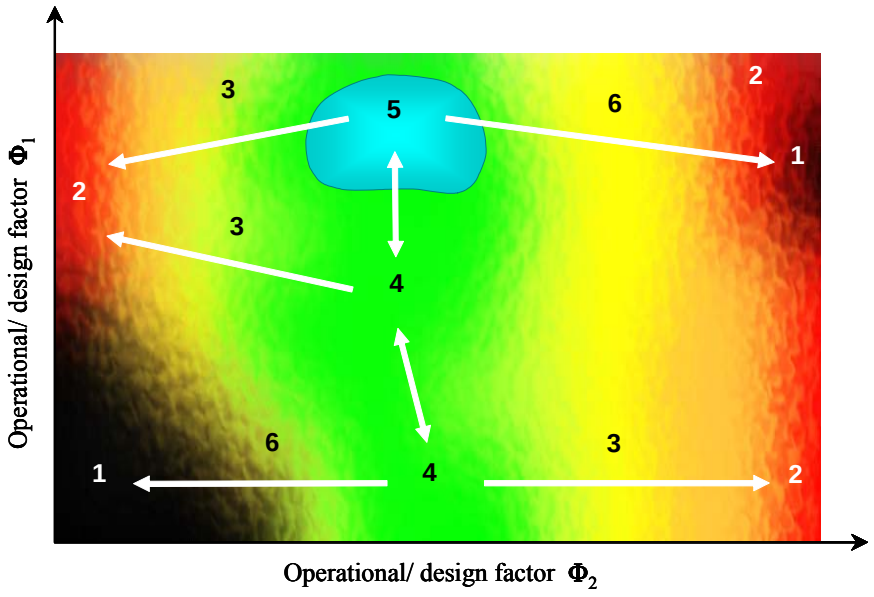


Legend: **1** – 'abyss' (catastrophe), **2** – 'hill' (danger), **3** – 'slope' (reversible state transitions), **4** – 'valley' (standard safety, norm), **5** – 'lake' (maximum safety/mission effectiveness, optimum), **6** –'precipice' (abrupt, irreversible state transitions, 'chain reaction').

| I | II-a | II-b | III | IV | V |
|---|---|---|---|---|---|

– safety classification categories

Fig. 4. Main objects of flight safety 'topology'

(a) Flight safety windows

(b) Safety chances distributions

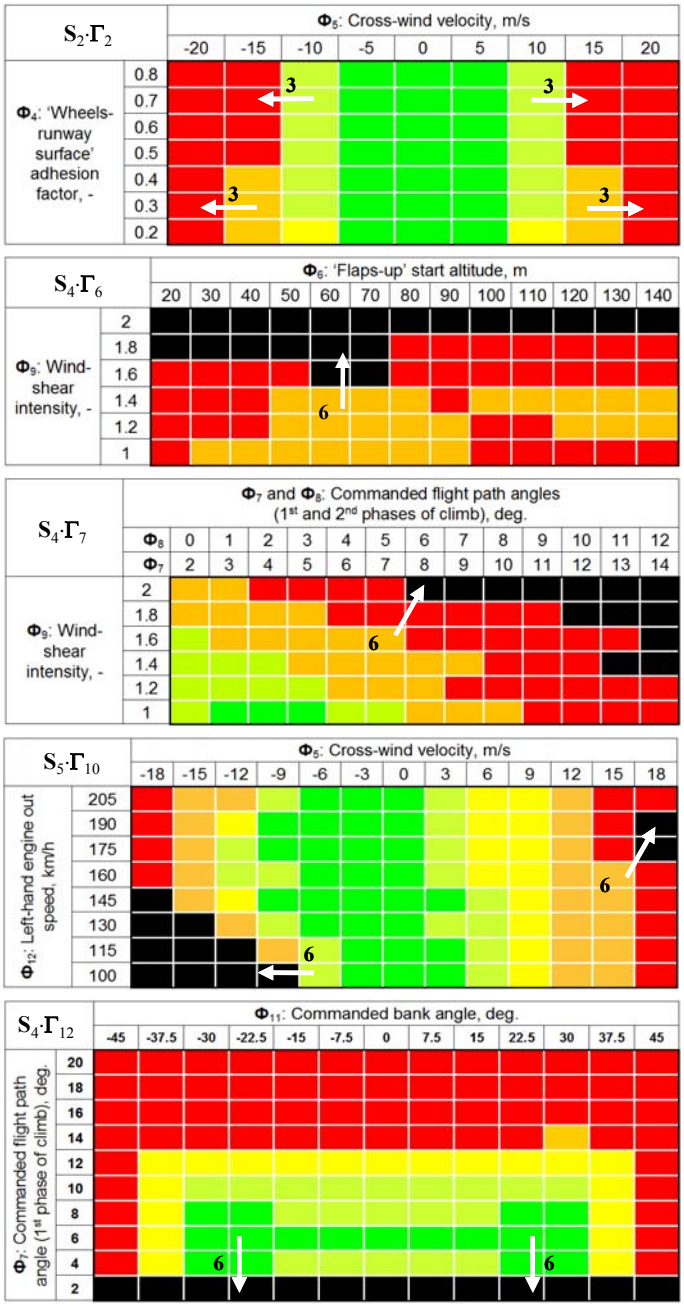


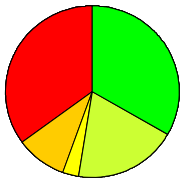

| Category | ξj | nj | χj, % |
|---|---|---|---|
| I | | 21 | 33 |
| II-a | | 12 | 19 |
| II-b | | 2 | 3 |
| III | | 6 | 10 |
| IV | | 22 | 35 |
| V | | 0 | 0 |
| Σnj, Σχj \| S2·Γ2: | | 63 | 100 |

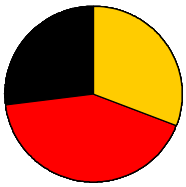

| Category | ξj | nj | χj, % |
|---|---|---|---|
| I | | 0 | 0 |
| II-a | | 0 | 0 |
| II-b | | 0 | 0 |
| III | | 24 | 31 |
| IV | | 33 | 42 |
| V | | 21 | 27 |
| Σnj, Σχj \| S4·Γ6: | | 78 | 100 |

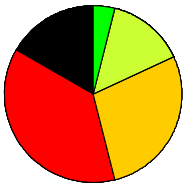

| Category | ξj | nj | χj, % |
|---|---|---|---|
| I | | 3 | 4 |
| II-a | | 11 | 14 |
| II-b | | 0 | 0 |
| III | | 22 | 28 |
| IV | | 29 | 37 |
| V | | 13 | 17 |
| Σnj, Σχj \| S4·Γ7: | | 78 | 100 |

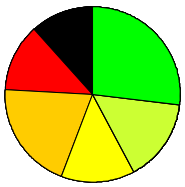

| Category | ξj | nj | χj, % |
|---|---|---|---|
| I | | 28 | 27 |
| II-a | | 16 | 15 |
| II-b | | 14 | 13 |
| III | | 21 | 20 |
| IV | | 13 | 13 |
| V | | 12 | 12 |
| Σnj, Σχj \| S5·Γ10 | | 104 | 100 |

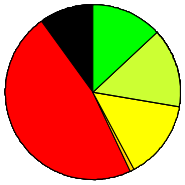

| Category | ξj | nj | χj, % |
|---|---|---|---|
| I | | 17 | 13 |
| II-a | | 19 | 15 |
| II-b | | 19 | 15 |
| III | | 1 | 1 |
| IV | | 61 | 46 |
| V | | 13 | 10 |
| Σnj, Σχj \| S4·Γ12 | | 130 | 100 |

Legend:

| | |
|---|---|
| $S_2 \cdot \Gamma_2$ | Normal takeoff in cross-wind conditions. Variations of cross-wind velocity and 'wheels – runway surface' adhesion factor |
| $S_4 \cdot \Gamma_6$ | Normal takeoff in wind-shear conditions. Variations of wind-shear intensity and errors in selecting 'flaps-up' start altitude |
| $S_4 \cdot \Gamma_7$ | Normal takeoff in wind-shear conditions, front C.G. position. Variations of wind-shear intensity and errors in maintaining commanded flight path angles (1st and 2nd phases of climb) |
| $S_5 \cdot \Gamma_{10}$ | Continued takeoff in cross-wind conditions with left-hand engine out during ground-roll. Variations of engine failure speed and cross-wind velocity |
| $S_4 \cdot \Gamma_{12}$ | Normal takeoff in 'strong' wind-shear conditions. Variations/errors in maintaining commanded flight path angle (1st phase of climb) and commanded bank angle |

Fig. 5. Flight safety windows (a) and safety chances distributions (b) for selected takeoff compositions $S_i \cdot \Gamma_k$

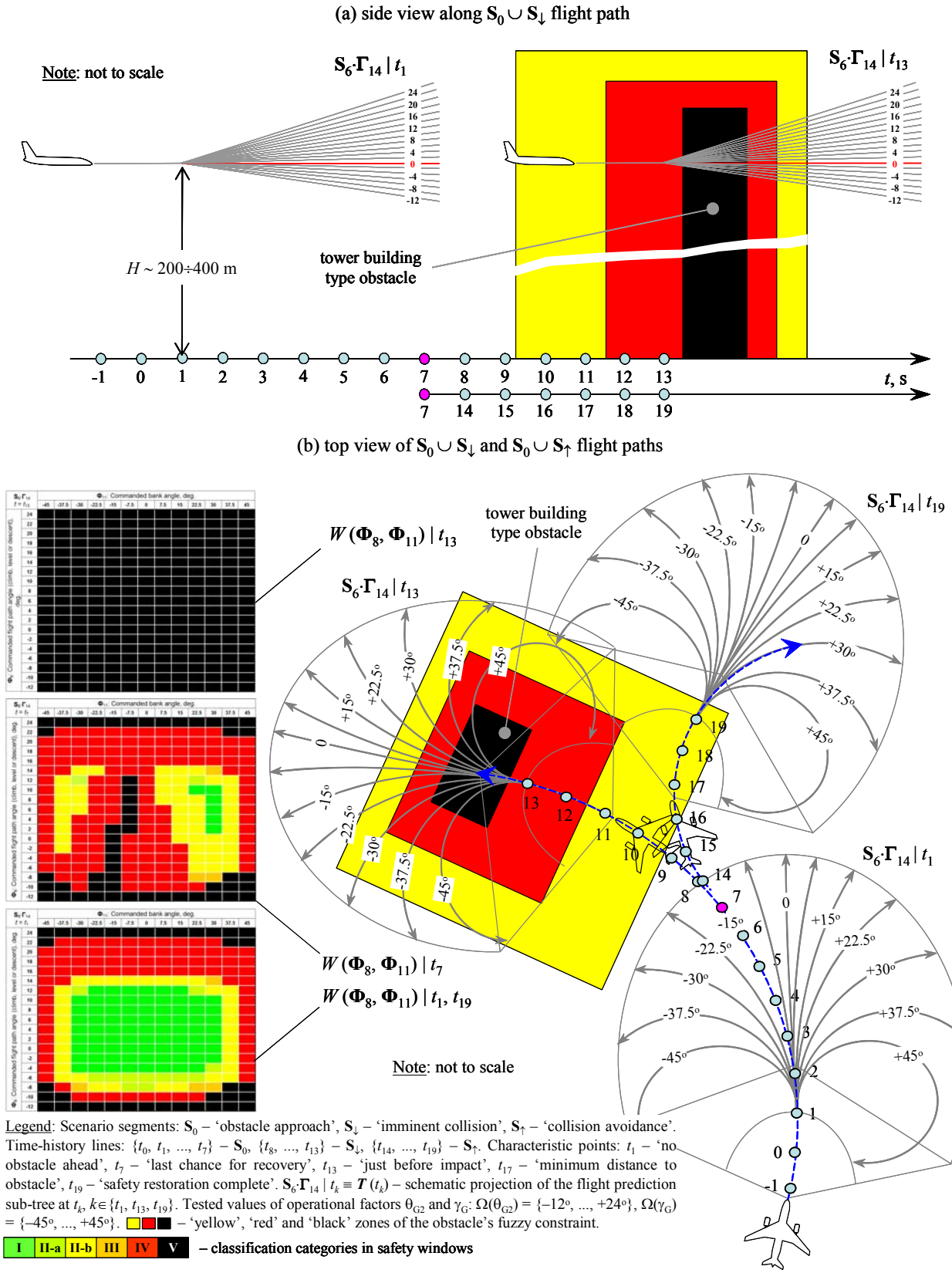


Legend: Scenario segments: $\mathbf{S}_0$ – 'obstacle approach', $\mathbf{S}_\downarrow$ – 'imminent collision', $\mathbf{S}_\uparrow$ – 'collision avoidance'. Time-history lines: $\{t_0, t_1, ..., t_7\}$ – $\mathbf{S}_0$, $\{t_8, ..., t_{13}\}$ – $\mathbf{S}_\downarrow$, $\{t_{14}, ..., t_{19}\}$ – $\mathbf{S}_\uparrow$. Characteristic points: $t_1$ – 'no obstacle ahead', $t_7$ – 'last chance for recovery', $t_{13}$ – 'just before impact', $t_{17}$ – 'minimum distance to obstacle', $t_{19}$ – 'safety restoration complete'. $\mathbf{S}_6{\cdot}\boldsymbol{\Gamma}_{14} \mid t_k \equiv \boldsymbol{T}(t_k)$ – schematic projection of the flight prediction sub-tree at $t_k$, $k \in \{t_1, t_{13}, t_{19}\}$. Tested values of operational factors $\theta_{G2}$ and $\gamma_G$: $\Omega(\theta_{G2}) = \{-12^o, ..., +24^o\}$, $\Omega(\gamma_G) = \{-45^o, ..., +45^o\}$. – 'yellow', 'red' and 'black' zones of the obstacle's fuzzy constraint.

Fig. 6. Flight path, situational tree and safety window states (selected) for two scenarios of low-altitude flight in the presence of urban obstacles ($\mathbf{S}_6{\cdot}\boldsymbol{\Gamma}_{14}$): $\mathbf{S}_0 \cup \mathbf{S}_\downarrow$ – terrorist-/ fool-type control, and $\mathbf{S}_0 \cup \mathbf{S}_\uparrow$ – safety protection AI control

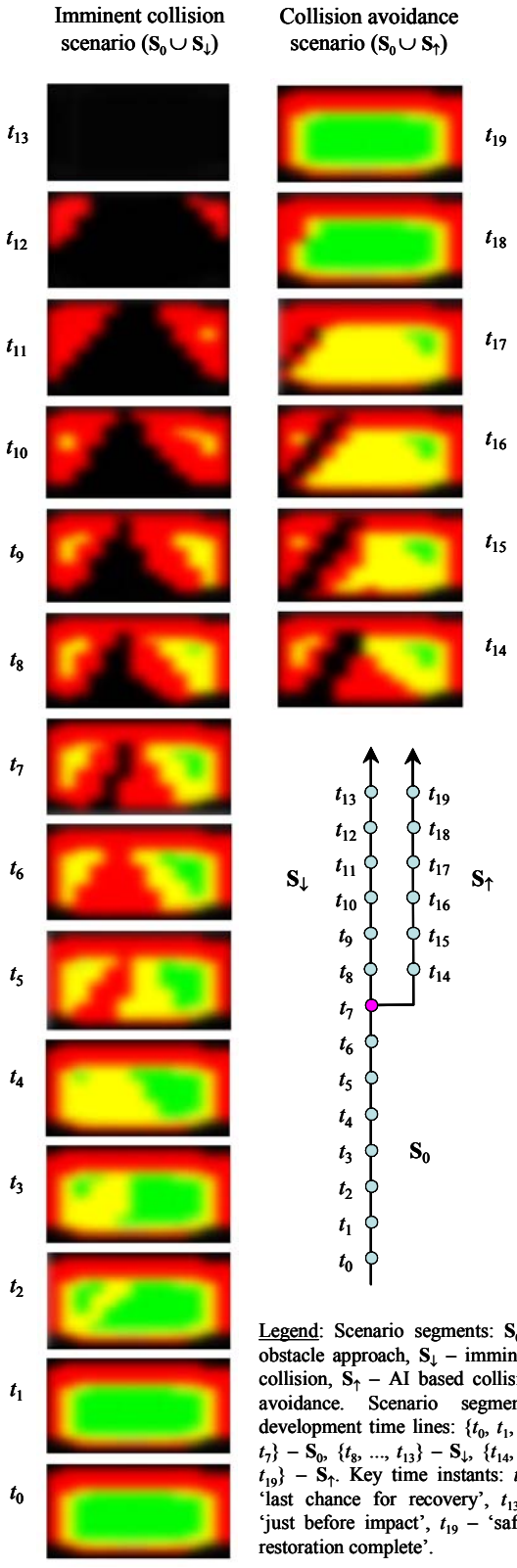


Legend: Scenario segments: $S_0$ – obstacle approach, $S_\downarrow$ – imminent collision, $S_\uparrow$ – AI based collision avoidance. Scenario segment's development time lines: $\{t_0, t_1, ..., t_7\} - S_0$, $\{t_8, ..., t_{13}\} - S_\downarrow$, $\{t_{14}, ..., t_{19}\} - S_\uparrow$. Key time instants: $t_7$ – 'last chance for recovery', $t_{13}$ – 'just before impact', $t_{19}$ – 'safety restoration complete'.

Fig. 7. Discrete time-history of fuzzified dynamic safety windows for two low-altitude flight scenarios in the presence of urban obstacles ($S_6 \cdot \Gamma_{14}$): $S_0 \cup S_\downarrow$ – imminent collision and $S_0 \cup S_\uparrow$ – collision avoidance

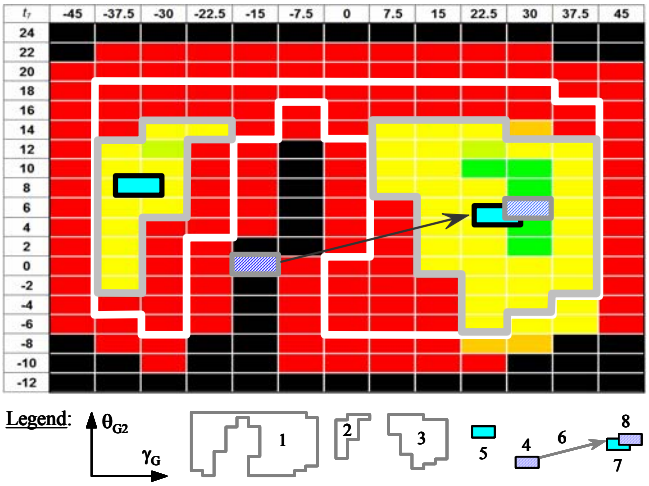


1 – zone of $\Delta\Phi$-secured non-catastrophic scenarios; 2, 3 – 'islands' of remaining safe/conditionally safe scenarios; 5, 7 – 'C.G.' locations for left- and right-hand 'islands' of remaining safe/conditionally safe scenarios; 4, 8 – old (catastrophe-prone) and new (safety restoring) value cells of the commanded flight path and bank angles, 6 – required shift of the commanded cell in the safety window.

Fig. 8. Key elements of the dynamic safety window for $S_6 \cdot \Gamma_{14}$ at the 'last chance for recovery' point $t_\uparrow \equiv t_7 : S_0 \rightarrow S_\uparrow$

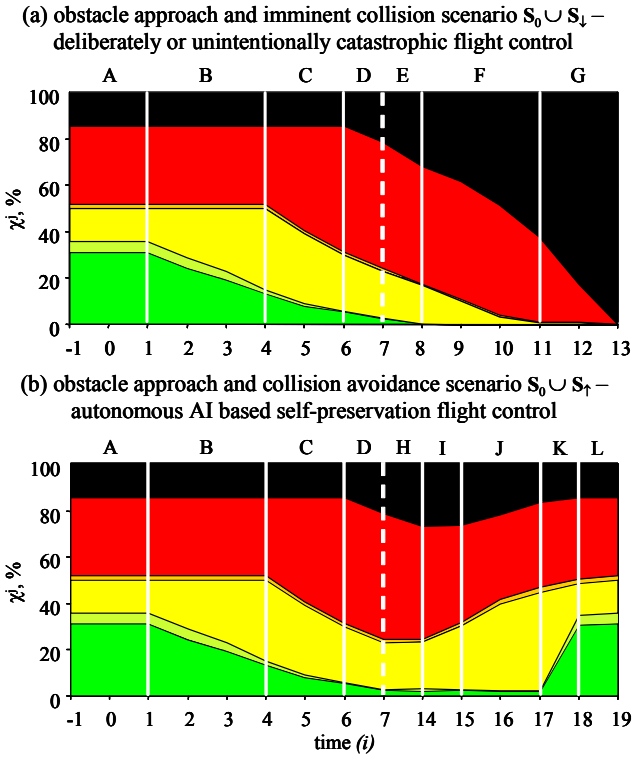


Legend: A, B, …, L - characteristic states of the aircraft safety dynamics; $\chi^j$ – flight safety chances at $\xi^j$ level, $j \in \{$**I**, **II-a**, **II-b**, **III**, **IV**, **V**$\}$; $t_i$ – time instants, $i \in \{-1, 0, 1, \ldots, 13\} \vee i \in \{-1, 0, 1, \ldots, 7, 14, 15, .., 19\}$.

Fig. 9. Time-history of safety chances distribution for two control tactics in low-altitude flight in the presence of urban infra-structure obstacles ($S_6 \cdot \Gamma_{14}$) – ref. Fig. 7: (a) terrorist-/fool-type control and (b) AI safety protection control